machines

MDPI

Article

Soft Robots: Computational Design, Fabrication, and Position Control of a Novel 3-DOF Soft Robot

Martin Garcia [1], Andrea-Contreras Esquen [1], Mark Sabbagh [2], Devin Grace [2], Ethan Schneider [2], Turaj Ashuri [3], Razvan Cristian Voicu [2], Ayse Tekes [1] and Amir Ali Amiri Moghadam [2,*]

[1] Department of Mechanical Engineering, Kennesaw State University, Marietta, GA 30060, USA; mgarci98@students.kennesaw.edu (M.G.); acontr14@students.kennesaw.edu (A.-C.E.); atekes@kennesaw.edu (A.T.)
[2] Department of Robotics and Mechatronics Engineering, Kennesaw State University, Marietta, GA 30060, USA; msabbag1@students.kennesaw.edu (M.S.); dgrace6@students.kennesaw.edu (D.G.); eschnei6@students.kennesaw.edu (E.S.); voicu@gatech.edu (R.C.V.)
[3] Office of the Dean, Kennesaw State University, Marietta, GA 30060, USA; tashuri@kennesaw.edu
* Correspondence: aamirimo@kennesaw.edu

Abstract: This paper presents the computational design, fabrication, and control of a novel 3-degrees-of-freedom (DOF) soft parallel robot. The design is inspired by a delta robot structure. It is engineered to overcome the limitations of traditional soft serial robot arms, which are typically low in structural stiffness and blocking force. Soft robotic systems are becoming increasingly popular due to their inherent compliance match to that of human body, making them an efficient solution for applications requiring direct contact with humans. The proposed soft robot consists of three soft closed-loop kinematic chains, each of which includes a soft actuator and a compliant four-bar arm. The complex nonlinear dynamics of the soft robot are numerically modeled, and the model is validated experimentally using a 6-DOF electromagnetic position sensor. This research contributes to the growing body of literature in the field of soft robotics, providing insights into the computational design, fabrication, and control of soft parallel robots for use in a variety of complex applications.

Keywords: delta soft robot; computational design; inverse kinematics of soft robots; KNN regression; neural network; uncertain Jacobian

Citation: Garcia, M.; Esquen, A.-C.; Sabbagh, M.; Grace, D.; Schneider, E.; Ashuri, T.; Voicu, R.C.; Tekes, A.; Amiri Moghadam, A.A. Soft Robots: Computational Design, Fabrication, and Position Control of a Novel 3-DOF Soft Robot. *Machines* **2024**, *12*, 539. https://doi.org/10.3390/machines12080539

Academic Editor: Dan Zhang

Received: 17 May 2024
Revised: 24 July 2024
Accepted: 1 August 2024
Published: 7 August 2024

1. Introduction

The emerging field of soft robotics derives much of its motivation from bioinspired designs of robotic systems that can safely interact with unknown environments [1–4]. Alongside the growth of soft robotics, the past decade has seen the development of numerous novel soft actuators and sensors [5]. These newly introduced transducer designs can function based on various actuation mechanisms such as pneumatic [6,7], hydraulic [8–10], thermal [11,12], electrical [13–15], and chemical [16–18].

Conventional rigid robotic systems heavily rely on applying force sensors and monitoring systems for interaction with humans. However, failure of such systems can be catastrophic, including harm and loss of life [19]. Inherent compliance match to the human body in soft robotic systems makes them among the best options for safe interaction with living systems. It is possible to engineer the structure of soft robotic systems such that the contact forces will always remain in a safe range in case of accidental collision with humans. Thus, it is possible to use soft robotic systems in a variety of applications, including medical [20–23], assistive technology [24–27], and search and rescue missions [28–32].

It is possible to break up safety compliance in robotic systems into two categories: active and passive. Active compliance in rigid robots utilizes sensory feedback force and torque data to control the position of the end-effector [33]. Feedback systems can be more complicated and require a rapid real-time response, limiting their application. On the other

hand, passive compliance is achievable by integrating soft compliance joints and links in the structure of the robot. Passive systems can deform under external forces, without requiring any sensory data or control system, to a safe limit for human–robot interactions.

However, passive-compliant systems suffer from low accuracy and complex dynamics. Most soft robotic systems include serial or hybrid structures, which limits their blocking force and accuracy. Soft parallel robots can address these shortcomings [19,34]. The research area of soft parallel robots is relatively new. Amiri Moghadam et al., for the first time in 2015, used the term "soft parallel robot" in their work on developing a 2-DOF soft parallel robot equipped with electroactive polymer actuators [35].

Since the field of soft parallel robots is a newly evolving discipline, it is important to categorize existing soft parallel robots to compare and understand their working principles better. One effective way to categorize these robots is based on the application of soft joints, links, or both soft joints and links.

We have utilized both soft links, and joints in 2-, 3-, and 6-DOF soft parallel robots [19,35,36]. There are several contributions for soft-link-only parallel robots [37–46]. Yang et al. have demonstrated the design and modeling of a soft-joint-only parallel robot inspired by the structure of delta robots [47].

In the current work, we propose a novel 3-DOF soft parallel robot that can move in the x, y, and z directions. The proposed soft robot is analogous to the rigid delta robot consisting of three soft active links connected to passive links and the robot platforms through soft joints. However, the very small scale and mass of the robot prototype and its soft links make it highly unlikely to injure people during operation as a medical device.

Compliant mechanisms utilize flexible hinges or flexible members to induce relative motion between neighboring links. Such mechanisms offer several advantages over rigid joint connections, including minimal friction loss, superior performance, and no need for assembly [48–50]. Additionally, it is possible to substantially increase a robot's workspace if compliant parts such as flexures or links are integrated into a soft robot's design [19].

The remainder of this paper is structured as follows. Section 2 details the design and fabrication of the proposed soft robot. Section 3 presents the modeling of the robot, encompassing both kinematics and dynamics. Finally, Section 4 provides the conclusions and future works.

2. Design and Fabrication

Rigid delta robots have wide adoption in systems requiring high-speed manipulation, such as pick and place tasks, using a pure axis of coordinate translation while preventing top plate rotation. Soft delta robots are designed by replacing the traditional revolute joints with their equivalent soft joints and replacing the active base links with soft actuators, as illustrated in Figure 1. thus allowing for increased workspace movement since the soft joints undergo large displacements when subjected to loading.

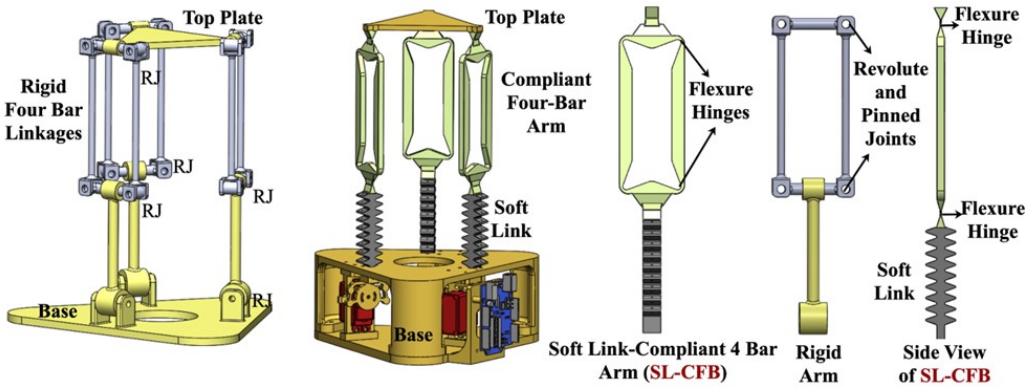

Figure 1. Design of rigid and soft delta robots. (RJ: revolute joint).

In contrast, revolute or pinned joints on the lower rigid links tend to exhibit limitations. Furthermore, designing and fabricating soft delta robots as a single piece is feasible, minimizing the number of parts and accessories while reducing manufacturing and assembly time.

The soft delta robot incorporates an active soft link connected to a passive upper compliant four-bar (CFB) arms through a flexure hinge called the single-soft link compliant four-bar arm (SL-CFB). The soft actuator links consist of a fin-like beam that allows for rotation and bending, emulating the motion of rigid bottom links. The single-piece CFB arm integrates flexure hinges, enabling side-to-side translation relative to the soft links. A servo motor with a pulley wheel that can pull a string in two directions actuates the tendon-driven soft links. The soft links bend inwards towards the center of the base with clockwise servo motor rotation. Conversely, rotating the servo contour-clockwise allows the soft links to bend outwards. Figure 2a demonstrates the bending configuration when the soft links are deflected outwards compared to the rotation on the rigid delta robot. Figure 2b shows the upper link lateral movement configuration with the upper link's translation to the left versus the rotation to the left on the rigid delta robot upper links.

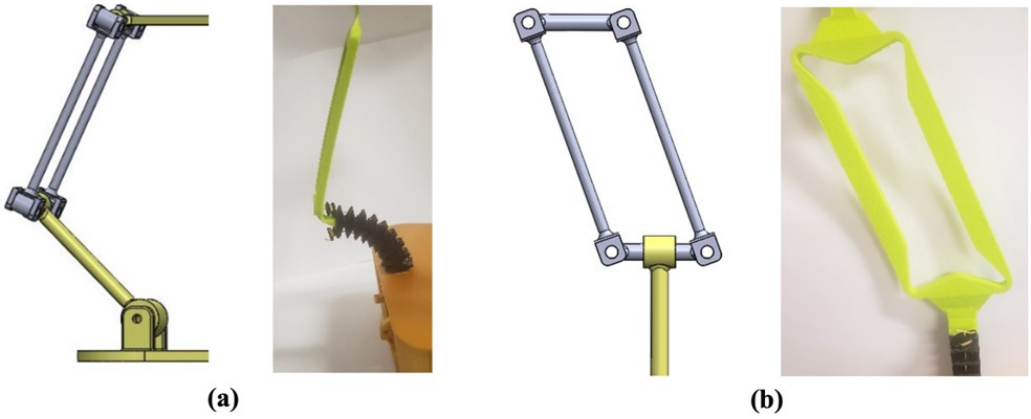

Figure 2. Comparison of (**a**) bending movement of rigid and soft links and (**b**) lateral movement of rigid and compliant upper links.

The main components of the soft delta robot are three SL-CFBs, a top plate, a bottom platform, three 20 kg servo motors (20 kg· cm of torque) to actuate the soft links through wires, wire string, and an embedded Arduino-based controller for the servo motor. Each soft link is encircled and separated by 120° on a triangular base, as depicted in Figure 3.

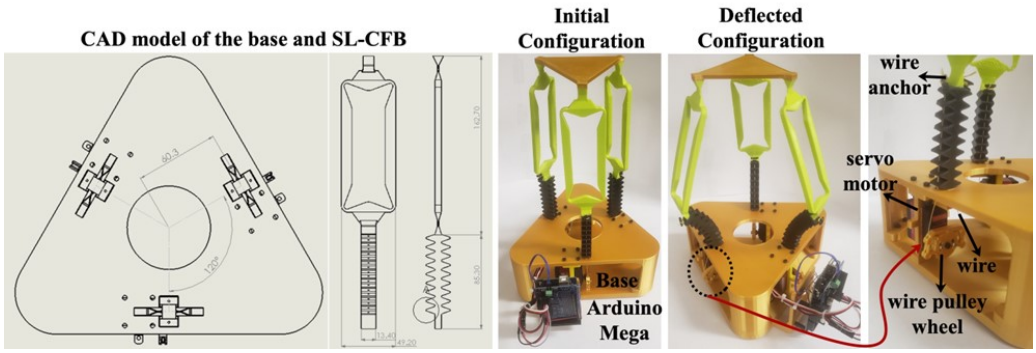

Figure 3. CAD model and the prototype of the proposed soft delta robot.

A single SL-CFB consists of an 85 mm long soft link and 163 mm long compliant four-bar arm with an overall length of 248 mm connected to the base and top plate. These dimensions are within the printing workspace of the 3D printer we used for this prototype. The upper compliant four-bar arms are 3D-printed using overture thermoplastic

polyurethane (TPU) filament at a 40% infill density. The soft links utilize NinjaFlex 3D printing and TPU filaments at 100% infill. The combination of the TPU and NinjaFlex materials provide the required flexibility for this design. The selection of infills is a trial-and-error process, with a tradeoff between the required flexibility for the soft design and the solidity to make it controllable.

The top plate, base platform, and servo mounts are 3D-printed using polylactic acid (PLA) filament. PLA provides a firm basis for the support of flexible delta robot links. The soft delta robot is controlled and programmed using the embedded controller with pulse-width modulation to operate the servo motor given a set trajectory. Each servo motor rotates a pulley wheel with two strings attached to the soft links via a 3D-printed anchor piece for optimal attachment. The experimental data are collected from the prototype soft delta robot using various sensors, including a TrakSTAR 6-degree-of-freedom position sensor. Figure 4 depicts the experimental setup. Figure 5 shows the working principle of tendon-driven actuators. These actuators consist of a soft backbone that can bend both clockwise and counterclockwise by pulling the tendons on either side using a servomotor.

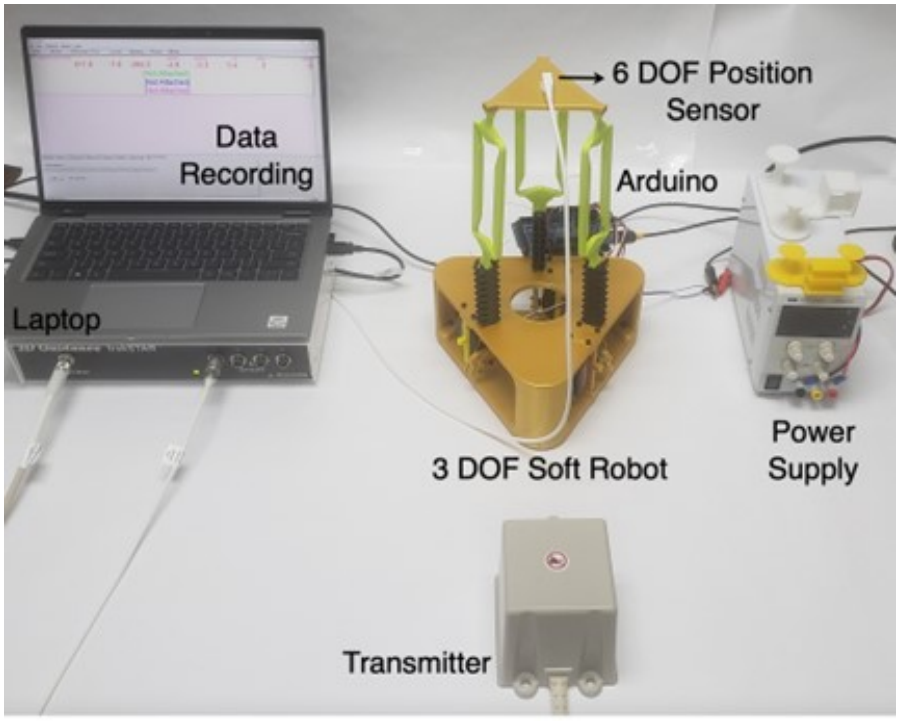

Figure 4. Experimental setup to prove the concept and validate the model.

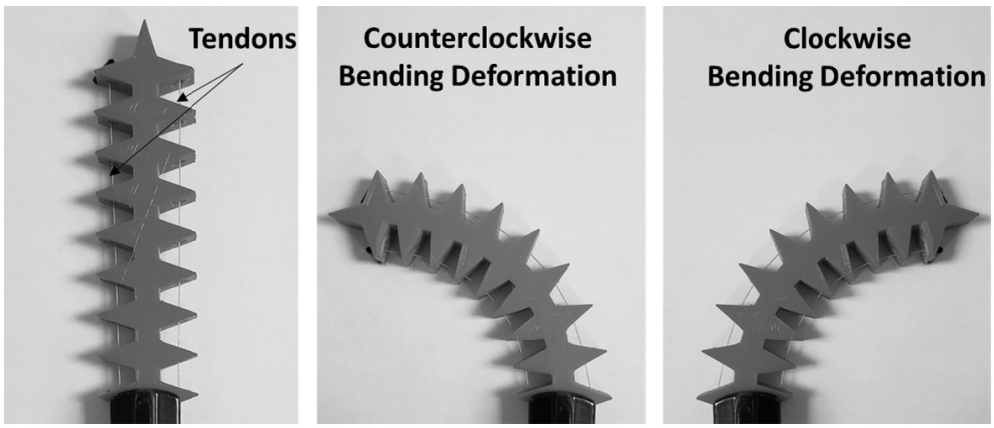

Figure 5. Working principle of tendon-driven actuators.

3. Modeling the Kinematics

We used two different modeling techniques for the kinematics of the soft robot. The first model is an analytical kinematic model. The second models is a numerical kinematic model that is developed in MATLAB Simscape. Since the robot incorporates soft base links and a compliant four-bar linkage designed as a single-piece arm, analytical modeling may not be accurate. MATLAB Simscape provides a platform for accurate modeling. Regulating the position of the top plate employs inverse kinematics for well-defined trajectories.

3.1. Analytic Kinematics

Kinematic analysis is necessary when designing robotic systems to provide a mapping that relates the end-effector position to the displacement of robot joints. Inverse and forward kinematics differ in the mapping direction. It is possible to obtain the soft robot's kinematics model assuming constant curvature for the motion of the 3D-printed tendon-driven actuators [2,24]. Afterward, assigning the proper frames to the soft robot platforms is possible. Figure 6 explains the kinematics model of the soft delta robot derived as follows.

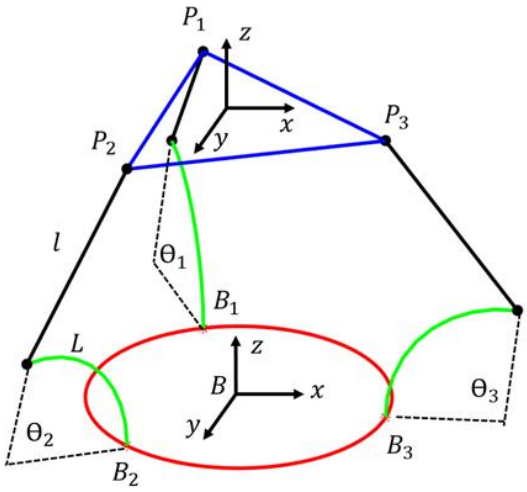

Figure 6. Frame assignment for the soft delta robot.

$$\{B_i^B\} + \{L_i^B\} + \{l_i^B\} = \{P_P^B\} + [R_P^B]\{P_i^P\} \quad i = 1, 2, 3. \tag{1}$$

B_i^B is the position of the vertex of the robot's fixed platform, L_i^B is the position of the soft actuators, l_i^B is the position of the passive links, P_P^B is the position of the end-effector, $[R_P^B]$ is the rotation matrix, and P_i^P is the positions of the vertices of the moving platform. Since the robot has 3 DOFs (x, y, z), the rotation matrix R is a unit matrix. The following equations provide the positions of the soft actuators:

$$\begin{aligned}
\{L_1^B\} &= \frac{L}{\theta_1}[\quad 0 \qquad\qquad \cos\theta_1 - 1 \qquad\quad \sin\theta_1]^T \\
\{L_2^B\} &= \frac{L}{\theta_2}[\frac{\sqrt{3}(1-\cos\theta_2)}{2} \qquad \frac{1-\cos\theta_2}{2} \qquad \sin\theta_2]^T \\
\{L_3^B\} &= \frac{L}{\theta_3}[\frac{\sqrt{3}(1-\cos\theta_3)}{2} \qquad \frac{1-\cos\theta_3}{2} \qquad \sin\theta_3]^T
\end{aligned} \tag{2}$$

L is the length of the soft actuators and θ_i is their bending angles. It is possible to rewrite Equation (1) as follows when considering the constant length of the passive links:

$$l_i = \left\|l_i^B\right\| = \left\|\{P_P^B\} + [R_P^B]\{P_i^P\} - \{B_i^B\} - \{L_i^B\}\right\| \quad i = 1, 2, 3. \tag{3}$$

It is beneficial to square the equation to avoid the square root in the norms of Equation (3).

$$l_i^2 = \left\| l_i^B \right\|^2 = l_{ix}^2 + l_{iy}^2 + l_{iz}^2 \quad i = 1, 2, 3. \tag{4}$$

Finally, solving Equation (4) numerically provides the value of the required bending angle in the active links for a given position of the robot end-effector.

We performed a workspace analysis using this developed kinematics model. A robot's workspace defines all the reachable points of the space for the robot end-effector, which establishes the applicability of the robot for a given task. The workspace helps in optimizing a robot's structure using the kinematic model to satisfy specific needs. Varying the robot's end-effector height from 90 mm to 160 mm and recording the maximum circular trajectory reach of the soft robot at each step aided in acquiring the robot workspace.

Figure 7 shows the workspace of the soft robot. It should be noted that the robot can follow any trajectory within the identified workspace. The choice of a circular trajectory is an arbitrary choice to show this capability within the feasible workspace.

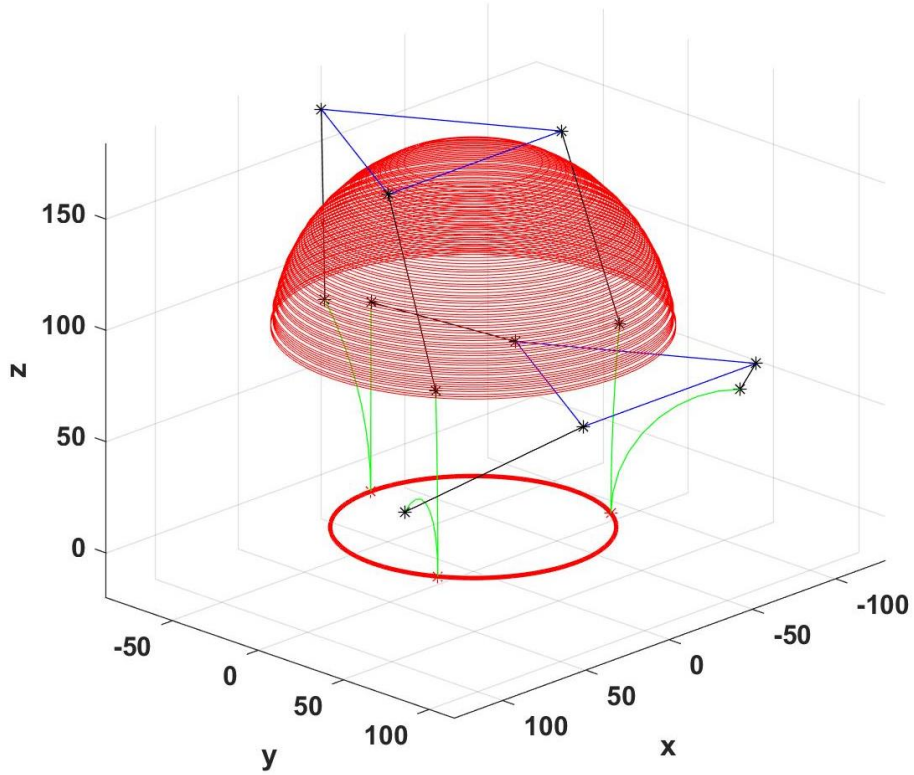

Figure 7. Workspace of the soft robot.

The soft robot simulation demonstrated the application of the kinematic model for horizontal and vertical trajectories before experimentally validating the results. Figure 8 shows the simulation results of the kinematics model for a horizontal trajectory and the required bending angles of the soft actuators.

Figure 9 depicts the simulation results for a vertical trajectory with the necessary bending angles of the soft actuators. The simulation results portray the kinematic model's effectiveness in predicting the soft robot's motion in different trajectories.

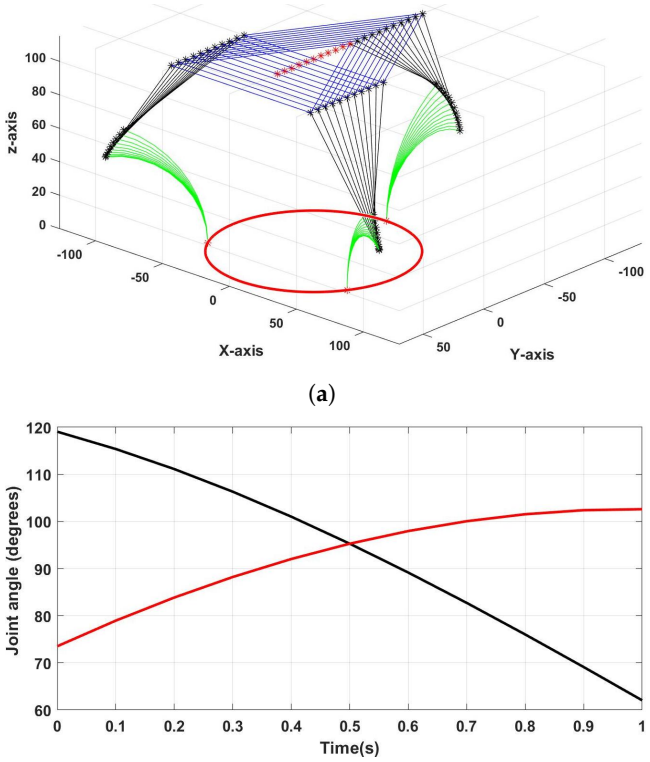

(**a**)

(**b**)

Figure 8. Kinematic model of the robot. (**a**) Horizontal trajectory; (**b**) joint angles.

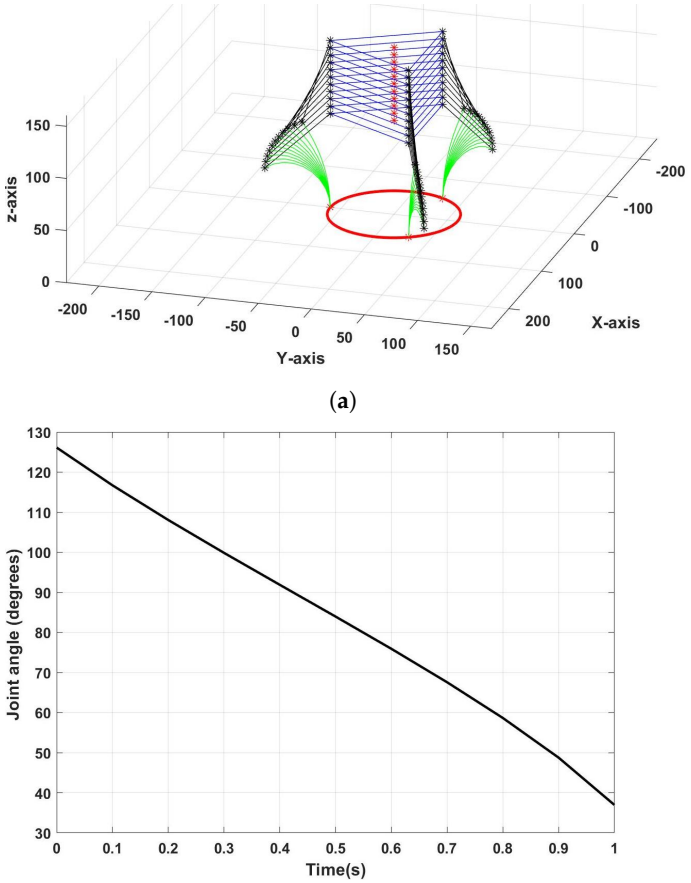

(**a**)

(**b**)

Figure 9. Kinematic model of the robot. (**a**) Vertical trajectory; (**b**) joint angles.

3.2. Numerical Kinematics

Simscape modeling is a low-fidelity technique that is beneficial due to its ease of design through the Simulink library blocks and CAD files. The SDOF soft link is created by alternating extruded solid blocks and revolute joint blocks oriented to allow inwards and outwards link curling, as seen in Figure 10a.

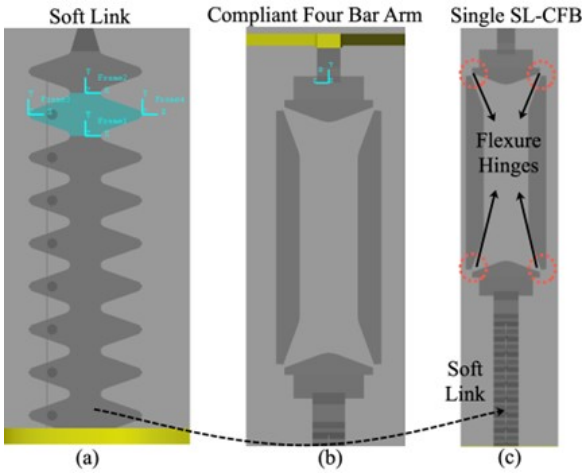

Figure 10. Simscape model of (**a**) soft link, (**b**) compliant four-bar, and (**c**) single SL-CFB.

Figure 10b shows the compliant four-bar arm made of extruded solids for the sides, revolute joints for the corners, and a gimbal joint that connects the rectangular piece to the tip. A pulley system and a motor provide the required tension in either direction for soft-link actuation.

The wire originates from a revolving cylindrical solid acting as the motor connected to each element of the flexible link using cylindrical solids and pulley blocks. Finally, the design ends at the last segment with a belt cable end block, illustrated in Figure 10a. Figure 10c depicts a single arm. Each cylindrical solid connects to a non-actuated revolute joint. The design includes three SL-CFB arms and motors connected to the base at the corresponding positions. The revolute joints representing the motors record the position or rotation angle as a time function, acting as sensors. Figure 11 illustrates the sensor data exported to the workspace in Simscape.

Actuating the soft robot is possible in two ways in the simulation. Like the physical robot, it is possible to actuate the motors by actuating the revolute joints connected to each soft link. Separately, it is possible to actuate the 6-DOF block attached to the center of the top plate. The torque is "automatically computed", and the actuation is "provided by input". A ramp signal provides the rotation angle, where a positive number moves the soft-link curl outward, and a negative number pulls the link inward. The simulation environment records the coordinates of the top plate in Simscape for experimental comparison.

Alternatively, to actuate via the 6-DOF joint connected to the top plate, the path of the top plate is generated for any desired trajectory and supplied as an input for the corresponding x, y, and z prismatic primitives. Through the simulation, obtaining the necessary angular displacements of the motor angles is essential to create the desired trajectory for the top plate.

We performed a validation and trajectory control to test the developed models. Experimental validation for the simulated soft robot confirmed the contributed findings. Figure 12 shows the validation of the Simscape model through experimental data.

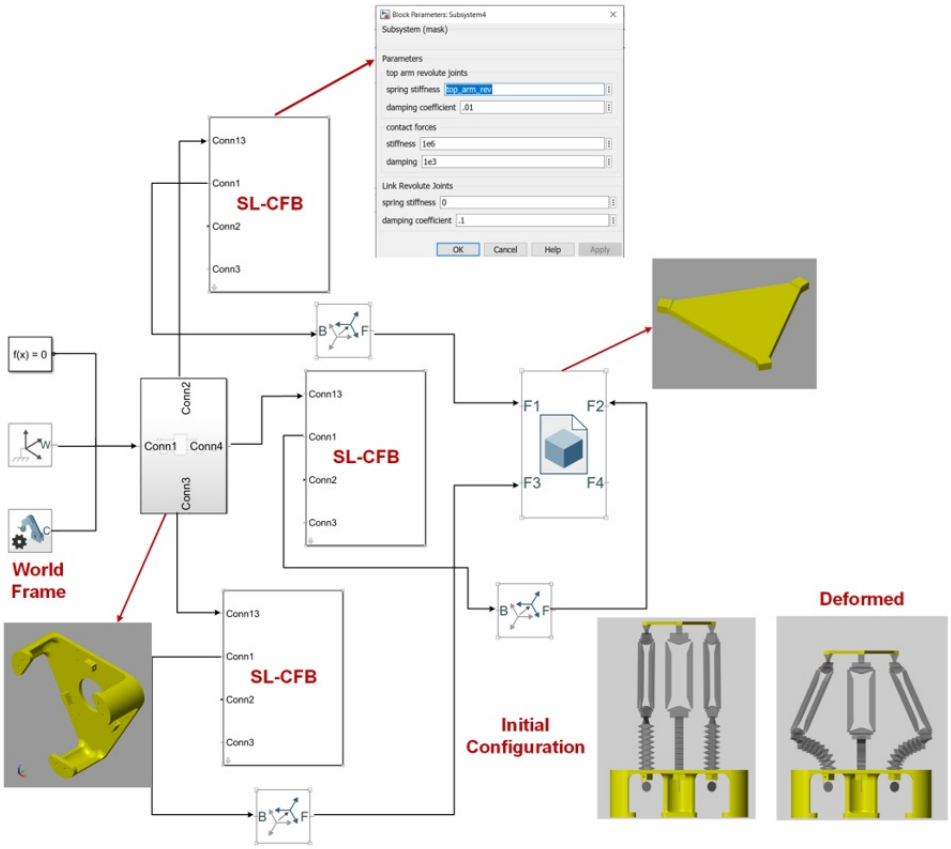

Figure 11. MATLAB Simscape model of the soft delta robot.

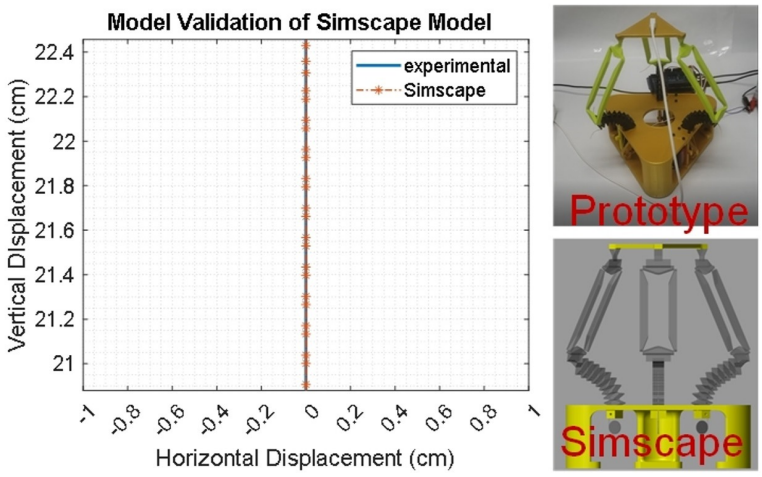

Figure 12. Validation of the Simscape model through experimental data.

Figures 13 and 14 provide the comparison results of the Simscape and experimental system responses for circular and spatial motion, respectively. The experimental setup includes the 3D-printed prototype and an NDI Aurora brand 6-DOF position sensor attached to the center of the top plate to record the position. This means that the rigid body, object, or system can move and rotate independently along all six axes in 3D space. This high degree of freedom enables tracking of complex movements and orientations, which is crucial for navigation inside the body. For instance, a robotic arm with six degrees of freedom can achieve a broader range of positions and orientations compared to systems with fewer degrees of freedom. The collected data processing utilizes MATLAB 9.13 with the NDI (ndigital.com) software to compare to the simulation model. Before running the experimen-

tal setup, sensor calibration was necessary to capture more accurate transmitter locations.

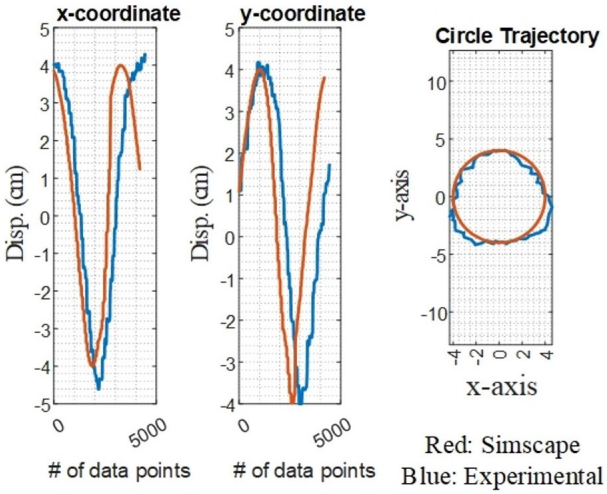

Figure 13. Comparison of Simscape and experimental system response for circular motion (planar trajectory).

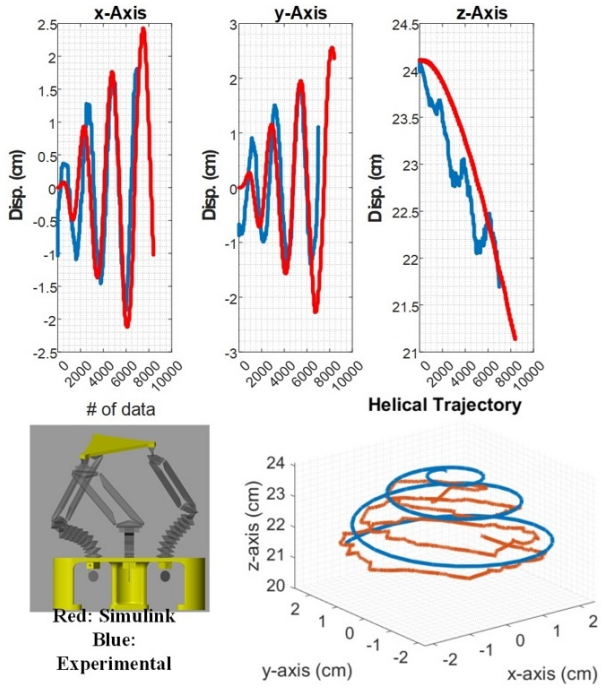

Figure 14. Comparison of Simscape and experimental system response for helical trajectory (spatial motion).

The validation results include bending the soft links outward by 68° in the same direction, ensuring the plate moves up and down while staying parallel to the surface without tilting. The same actuation input was applied to the Simscape model and recorded for top-plate-coordinate comparison. The Simscape model responded the same as the prototype.

After the numerical validation, planar circular and 3D helical motion trajectories are created based on Equation (5). The coordinates are provided as input displacements to the top plate's center to extract the base links' corresponding angular deflections from the Simscape model.

$$\begin{aligned} x = r \times \cos(\theta), \quad y = r \times \sin(\theta), \quad z = z_{initial} \\ x(t) = \sin(t) \times \cos(\omega t) \\ y(t) = \sin(t) \times \cos(\omega t) \\ z(t) = \cos(t) + z_{initial} \end{aligned} \tag{5}$$

The top plate can follow any desired trajectory through the deflections of the flexure hinges of the compliant four-bar arm only, without the requirement of bending on the soft links in Simscape. However, the physical system actuation is only possible using the motors to bend the soft links outwards or inwards. Overcoming this limitation is possible by initial lowering of the top platform in the simulation to permit further desired motion via the deformation of the soft links, specifically for circular motion, since a helical trajectory already possesses vertical displacement.

Afterward, validation is possible by applying the angular displacements obtained from the Simscape as inputs for the motors actuating in the physical testbed. Figures 10 and 11 provide the tendon results. The prototype follows the same trajectories extracted from the Simscape model with a slight deviation. One of the reasons might be how the 6-DOF position sensor was attached to the plate. This is due to the fact that the attachment of the sensor to the plate is subject to some minor misalignment from the ideal location and orientation used for experiments.

4. Soft Robot Position Control

This section addresses the challenges of controlling soft robots in the real world and experimental environments to gather results. It is difficult to design a controller subject to uncertainties such as materials, geometry, and input loading [51–54]. The soft parallel manipulator in this study has an uncertain Jacobian that makes traditional control methods challenging to implement. Furthermore, simulations often need to be faster to run in real time, limiting their usefulness for control purposes.

To overcome these challenges, the experimental testbed utilizes a data-driven approach to perform inverse kinematics. Instead of relying on a Jacobian, the joint changes based on the inverse kinematics of the real-world position are estimated compared to the desired position. The experiments implement two test methods: a neural network approach and a k-nearest neighbors (KNN) regression approach.

4.1. Data-Driven Approaches in Control

Data-driven approaches have a wide range of applications in control systems engineering [55–58]. In robotic systems, inverse kinematics is a critical problem, particularly for soft manipulators subject to nonlinearity, elasticity, and other complex factors. Recent research has explored using data-driven methods to learn accurate and nonlinearity-compensated inverse kinematics models for these manipulators. One such approach is k-nearest neighbors regression (KNNR), which can be an efficient and effective alternative to numerical solutions [59–61].

In a study by Zhang et al., KNNR was applied to the problem of learning inverse kinematics for a tendon-driven serpentine manipulator (TSM) [62]. The high nonlinearities caused by cable tensioning, elastic elements, and interaction of adjacent joints in the serpentine structure make TSM a particularly challenging platform for inverse kinematics modeling. Zhang et al. found that KNNR outperformed other methods, including Gaussian mixture regression and extreme learning machine, with the lowest root mean square error in tracking experiments [63].

The use of KNNR in robotics has been studied in multiple studies in the past. For example, Fuppeteer, a wearable 6-DOF display for delivering fingertip tactile cues, required inverse kinematics interpolation to achieve positions and orientations in the continuous workspace of the device [64]. Different interpolation methods, including KNNR, were evaluated on 1000 random poses. The KNNR-method-estimated leg lengths as a weighted average of k-nearest neighbors demonstrated its potential for data-driven kinematics of robots.

Neural network-based approaches have become increasingly popular for a wide range of engineering applications [65–67], including robotic control, by compensating for unknown variables [68–71]. Zhang et al. employed a neural network model to enhance robot position control using force information [63]. The approach used multiple factors such as movement trajectory, speed, shape, length, and material as input data for the neural network model.

Shao et al. proposed an improved neural network adaptive control (INNAC) method to regulate the bending angle of each finger of a hand rehabilitation robot driven by flexible pneumatic muscles [72]. The application exhibited a better control effect and stability than single neuron network adaptive control (SNNAC). Bamgbose et al. developed a data-driven approach to controller design for autonomous systems using a neural network-optimized control scheme based on samples from test navigation, which did not require precise models of the plant [73]. The implementation was effective in terms of faster transient response and overall error minimization in two case studies, one involving mobile robot motion control and the other involving the pitch and yaw angle control of a 2-DOF helicopter.

Majumdar et al. synthesized a neural network-based gain-scheduled proportional–integral–derivative (PID) controller to regulate the position of a pneumatic artificial muscle [74]. The proposed controller exhibited superior performance to classical PID controllers, with fast convergence, minimum oscillations, and reduced steady-state error. Ding et al. presented a neural network-based hybrid position and force-tracking control strategy for a robot model [75]. The proposed control scheme guaranteed both position-tracking accuracy and force-tracking capability, making it suitable for industrial scenarios that require precise force control and frequent force switching.

Wang et al. studied a control strategy for a planar underactuated manipulator system based on a wavelet neural network (WNN) model to achieve the position control objective of the system [76]. The study found that the proposed control scheme effectively achieved the position control objective of the system.

Overall, these studies highlight the potential of KNNR and neural networks for solving inverse kinematics problems in robotics, particularly for soft manipulators with high nonlinearities. By leveraging data-driven methods, KNNR and NN offer efficient and effective alternatives to traditional analytical kinematics models, enabling more precise and accurate motion control for these complex systems.

The present study employed a fundamental neural network control strategy to achieve position control. The network we employed, shown in Figure 15, consisted of a three-input and three-output model with three hidden layers, containing 9, 27, and 9 nodes, respectively.

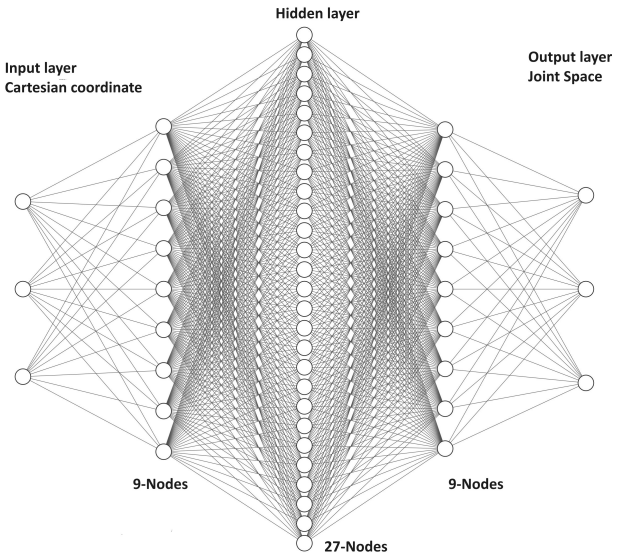

Figure 15. Neural network structure.

The inputs are the Cartesian coordinates (x, y, z) of the moving platform with respect to the home position and the outputs are the three motor angles. To train the network, we utilized a comprehensive dataset comprising 226,983 observations of the correlation between motor degrees and position. Additionally, we employed the k-nearest neighbors (KNN) algorithm using the same dataset. Although the KNN algorithm does not require explicit training, we still had to tune the k-value, i.e., the number of neighbors involved in the estimation of motor positions. Our KNN algorithm uses a k-value of 15.

4.2. Closed-Loop Position Control

In traditional control loops, the Jacobian matrix helps relate the end-effector's velocities to the joints' velocities [77]. However, the uncertain Jacobian makes traditional control methods challenging for soft parallel manipulators like the one studied in this research [78,79]. Moreover, the analytical model used for simulations lacks real-time performance, rendering it unsuitable for the control loop. Hence, a data-driven approach to perform inverse kinematics (IK) and estimate joint changes facilitates the implementation.

A control loop implementation aids in achieving real-time control for the soft parallel manipulator, as shown in Figure 16. The control loop takes in the target position and feeds it into an inverse kinematics (IK) solver to calculate the desired angles for the servos.

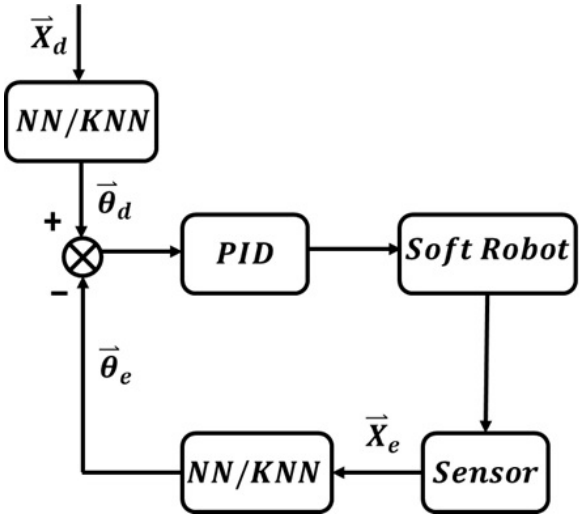

Figure 16. Closed-loop control using PID and NN/KNN as kinematic model.

The desired angles are then compared to the expected angles based on the real-world position obtained from the 6-DOF sensor, producing an angle error. The angle error is updated with a proportional–integral–derivative (PID) controller to estimate the required servo movements to compensate for the position error. This approach overcomes the challenges associated with the uncertain Jacobian of the manipulator while also providing real-time performance.

4.3. Experimental Position Control Results

This article presents a series of open- and closed-loop control experiments to evaluate the soft parallel manipulator's performance. The open-loop tests implement three approaches: the kinematic model assuming circular curvature, KNN regression, and neural network. Figure 17a–c depict the results, where the red trajectory represents the target trajectory, and the blue trajectory represents the actual position recorded by the 6-DOF sensor.

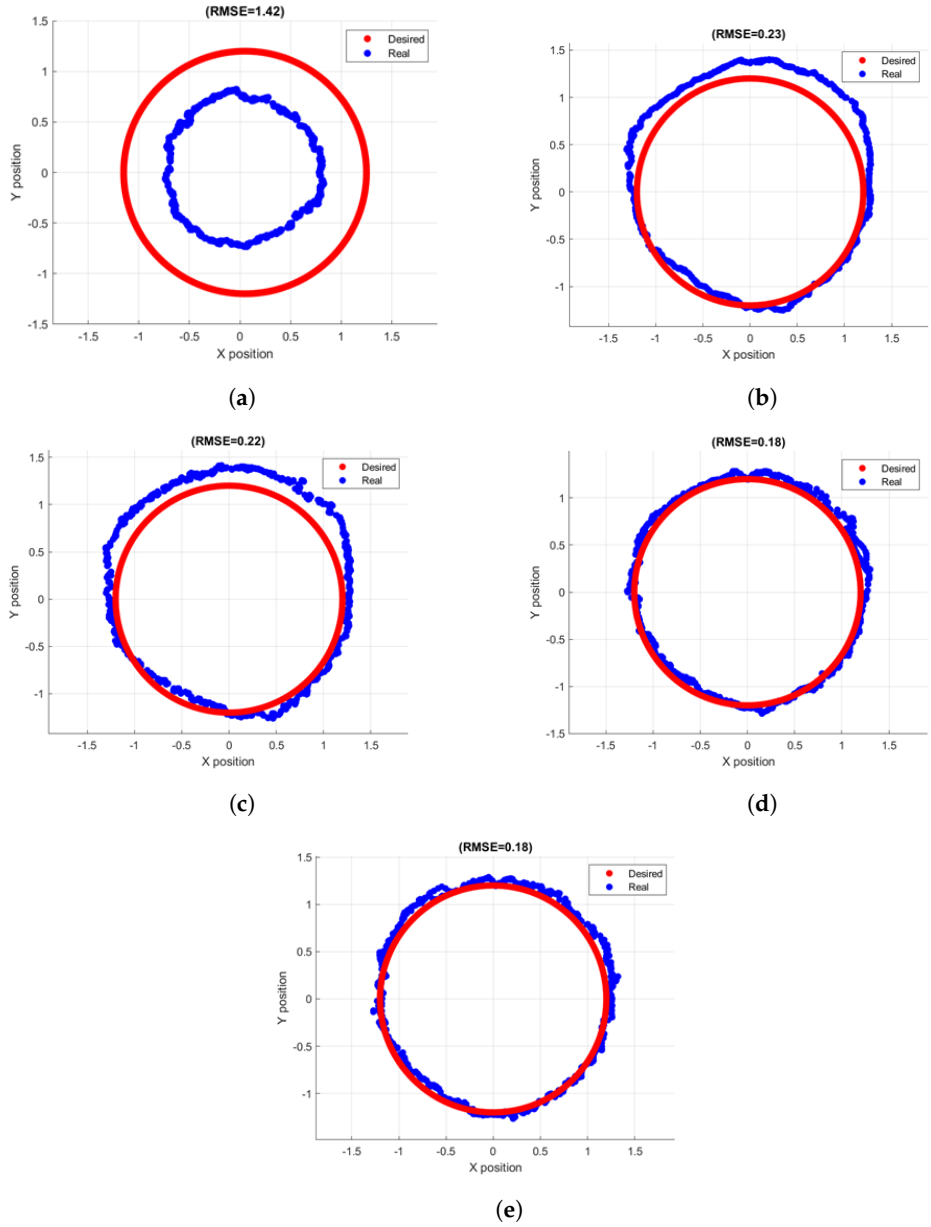

Figure 17. Open- and closed-loop responses. (**a**) Analytical model, open loop; (**b**) KNN regression, open loop; (**c**) neural network, open loop; (**d**) KNN regression, closed loop; (**e**) neural network, closed loop.

It is important to note that all measurements utilizing the kinematic model had the poorest performance among the open-loop tests, with a root-mean-square error (RMSE) of 1.46. Optimizing the parameters for the specific trajectory can improve the performance of the kinematic model. In contrast, the neural network controller and the KNN regression controller performed similarly, producing RMSE values of 0.16 and 0.19, respectively.

Figure 17d,e show the KNN regression and neural network results in the closed-loop (PID controller) experiment tests. Both controllers produced an RMSE of 0.08, showcasing the effectiveness of the data-driven approach in compensating for the uncertain Jacobian and improving the control of the soft parallel manipulator.

5. Conclusions

This paper reports on the design, modeling, and fabrication of a novel 3-DOF soft parallel robot analogous to a rigid delta robot. The robot consists of three closed kinematic chains connecting the top moving platform to the bottom through soft active/passive links

and joints. The kinematics model of the robot is derived based on the constant curvature assumption and used to obtain its typical workspace. The robot's structure was 3D-printed using TPU and NinjaFlex and actuated through three tendon-driven soft actuators.

The kinematic models showed that the robot could move in arbitrary 3D trajectories within its workspace. The model of the soft robot is simulated using Simscape. Simulating the motion of the soft links includes using discrete sets of elements connected using rotary joints and springs in the modeling. Comparing the experimental data and simulation results indicates the effectiveness of the design and Simscape model. Future work includes robust position control of the soft robot and more optimal soft robots with six DOFs.

Author Contributions: Writing—original draft, M.S., D.G., E.S., T.A., R.C.V., A.T. and A.A.A.M.; Writing—review & editing, M.G. and A.-C.E.; Supervision, A.A.A.M. All authors have read and agreed to the published version of the manuscript.

Funding: The research reported in this publication was supported by the National Institute of Biomedical Imaging and Bioengineering of the National Institutes of Health under Award Number R15EB032189. The content is solely the responsibility of the authors and does not necessarily represent the official views of the National Institutes of Health.

Data Availability Statement: Data are contained within the article.

Conflicts of Interest: The authors declare no conflicts of interest.

References

1. Hawkes, E.W.; Majidi, C.; Tolley, M.T. Hard questions for soft robotics. *Sci. Robot.* **2021**, *6*, eabg6049. [CrossRef] [PubMed]
2. Kim, S.; Laschi, C.; Trimmer, B. Soft robotics: A bioinspired evolution in robotics. *Trends Biotechnol.* **2013**, *31*, 287–294. [CrossRef]
3. Papendorp, S.; Ovando, A.; Gharaie, S.; Mosadegh, B.; Guerra-Zubiaga, D.; Alaie, S.; Ashuri, T.; Moghadam, A.A.A. Toward Development of Novel Remote Ultrasound Robotic System Using Soft Robotics Technology. *J. Eng. Sci. Med. Diagn. Ther.* **2024**, *7*, 021012. [CrossRef] [PubMed]
4. Gilmore, J.; Abidoye, C.; Grace, D.; Voicu, R.C.; Ashuri, T.; Moghadam, A.A.A. Development of Novel Stewart Robot Equipped with 3D Printed Soft Actuators. In Proceedings of the SoutheastCon 2024 Atlanta, GA, USA, 15–24 March 2024; IEEE: Piscataway, NJ, USA, 2024; pp. 960–965.
5. Ashuri, T.; Armani, A.; Jalilzadeh Hamidi, R.; Reasnor, T.; Ahmadi, S.; Iqbal, K. Biomedical soft robots: Current status and perspective. *Biomed. Eng. Lett.* **2020**, *10*, 369–385. [CrossRef]
6. Walker, J.; Zidek, T.; Harbel, C.; Yoon, S.; Strickland, F.S.; Kumar, S.; Shin, M. Soft robotics: A review of recent developments of pneumatic soft actuators. *Actuators* **2020**, *9*, 3. [CrossRef]
7. Papendorp, S.; Iyun, O.; Schneider, C.; Tekes, A.; Ashuri, T.; Amiri Moghadam, A.A. Development of 3d Printed Soft Pneumatic Hand Motion Sensors. In Proceedings of the ASME International Mechanical Engineering Congress and Exposition, Columbus, OH, USA, 30 October–3 November 2022; American Society of Mechanical Engineers: New York, NY, USA, 2022; Volume 86663, p. V004T05A067.
8. Chen, G.; Yang, X.; Zhang, X.; Hu, H. Water hydraulic soft actuators for underwater autonomous robotic systems. *Appl. Ocean Res.* **2021**, *109*, 102551. [CrossRef]
9. Katzschmann, R.K.; Marchese, A.D.; Rus, D. Hydraulic autonomous soft robotic fish for 3D swimming. In Proceedings of the Experimental Robotics: The 14th International Symposium on Experimental Robotics, Essaouira, Morocco, 15–18 June 2014; Springer: Berlin/Heidelberg, Germany, 2015; pp. 405–420.
10. Katzschmann, R.K.; De Maille, A.; Dorhout, D.L.; Rus, D. Cyclic hydraulic actuation for soft robotic devices. In Proceedings of the 2016 IEEE/RSJ International Conference on Intelligent Robots and Systems (IROS), Daejeon, Republic of Korea, 9–14 October 2016; IEEE: Piscataway, NJ, USA, 2016; pp. 3048–3055.
11. Wu, S.; Baker, G.L.; Yin, J.; Zhu, Y. Fast Thermal Actuators for Soft Robotics. *Soft Robot.* **2021**, *9*, 1031–1039. [CrossRef]
12. Hu, F.; Lyu, L.; He, Y. A 3D printed paper-based thermally driven soft robotic gripper inspired by cabbage. *Int. J. Precis. Eng. Manuf.* **2019**, *20*, 1915–1928. [CrossRef]
13. Acevedo-Velazquez, A.I.; Keshtkar, N.; Mersch, J.; Katzer, K.; Cherif, C.; Zimmermann, M.; Gerlach, G.; Röbenack, K. Construction, modeling, and control of a three-beam prototype using interactive fiber rubber composites. *PAMM* **2023**, *23*, e202300198. [CrossRef]
14. Song, K.; Kim, S.; Cha, Y. Soft electromagnetic actuator for assembly robots. *Smart Mater. Struct.* **2020**, *29*, 067001. [CrossRef]
15. Ovando, A.; Papendorp, S.; Ashuri, T.; Amiri Moghadam, A.A. Development of a Novel Hybrid Soft Cable-Driven Parallel Robot. In Proceedings of the ASME International Mechanical Engineering Congress and Exposition, New Orleans, LA, USA, 29 October–2 November 2023; American Society of Mechanical Engineers: New York, NY, USA, 2023; Volume 87622, p. V005T06A059.
16. Villeda-Hernandez, M.; Baker, B.C.; Romero, C.; Rossiter, J.M.; Dicker, M.P.; Faul, C.F. Chemically driven oscillating soft pneumatic actuation. *Soft Robot.* **2023**, *10*, 1159–1170. [CrossRef] [PubMed]

17. Onal, C.D.; Chen, X.; Whitesides, G.M.; Rus, D. Soft mobile robots with on-board chemical pressure generation. In Proceedings of the Robotics Research: The 15th International Symposium ISRR, Flagstaff, AZ, USA, 9–12 December 2011; Springer: Berlin/Heidelberg, Germany, 2017; pp. 525–540.
18. Liao, W.; Yang, Z. The integration of sensing and actuating based on a simple design fiber actuator towards intelligent soft robots. *Adv. Mater. Technol.* **2022**, *7*, 2101260. [CrossRef]
19. Garcia, M.; Pena, P.; Tekes, A.; Moghadam, A.A.A. Development of Novel Three-Dimensional Soft Parallel Robot. In Proceedings of the SoutheastCon 2021, Atlanta, GA, USA, 10–13 March 2021; IEEE: Piscataway, NJ, USA, 2021; pp. 1–6.
20. Hsiao, J.H.; Chang, J.Y.; Cheng, C.M. Soft medical robotics: Clinical and biomedical applications, challenges, and future directions. *Adv. Robot.* **2019**, *33*, 1099–1111. [CrossRef]
21. Banerjee, H.; Tse, Z.T.H.; Ren, H. Soft robotics with compliance and adaptation for biomedical applications and forthcoming challenges. *Int. J. Robot. Autom* **2018**, *33*, 68–80. [CrossRef]
22. Cianchetti, M.; Laschi, C.; Menciassi, A.; Dario, P. Biomedical applications of soft robotics. *Nat. Rev. Mater.* **2018**, *3*, 143–153. [CrossRef]
23. Sitti, M. Miniature soft robots—Road to the clinic. *Nat. Rev. Mater.* **2018**, *3*, 74–75. [CrossRef]
24. Oguntosin, V.; Harwin, W.S.; Kawamura, S.; Nasuto, S.J.; Hayashi, Y. Development of a wearable assistive soft robotic device for elbow rehabilitation. In Proceedings of the 2015 IEEE International Conference on Rehabilitation Robotics (ICORR), Singapore, 11–14 August 2015; IEEE: Piscataway, NJ, USA, 2015; pp. 747–752.
25. Manti, M.; Pratesi, A.; Falotico, E.; Cianchetti, M.; Laschi, C. Soft assistive robot for personal care of elderly people. In Proceedings of the 2016 6th IEEE International Conference on Biomedical Robotics and Biomechatronics (BioRob), Singapore, 26–29 June 2016; IEEE: Piscataway, NJ, USA, 2016; pp. 833–838.
26. Ansari, Y.; Manti, M.; Falotico, E.; Mollard, Y.; Cianchetti, M.; Laschi, C. Towards the development of a soft manipulator as an assistive robot for personal care of elderly people. *Int. J. Adv. Robot. Syst.* **2017**, *14*, 1729881416687132. [CrossRef]
27. Shahid, T.; Gouwanda, D.; Nurzaman, S.G.; Gopalai, A.A. Moving toward soft robotics: A decade review of the design of hand exoskeletons. *Biomimetics* **2018**, *3*, 17. [CrossRef]
28. Hawkes, E.W.; Blumenschein, L.H.; Greer, J.D.; Okamura, A.M. A soft robot that navigates its environment through growth. *Sci. Robot.* **2017**, *2*, eaan3028. [CrossRef]
29. der Maur, P.A.; Djambazi, B.; Haberthür, Y.; Hörmann, P.; Kübler, A.; Lustenberger, M.; Sigrist, S.; Vigen, O.; Förster, J.; Achermann, F.; et al. Roboa: Construction and evaluation of a steerable vine robot for search and rescue applications. In Proceedings of the 2021 IEEE 4th International Conference on Soft Robotics (RoboSoft), New Haven, CT, USA, 12–16 April 2021; IEEE: Piscataway, NJ, USA, 2021; pp. 15–20.
30. Mintchev, S.; Zappetti, D.; Willemin, J.; Floreano, D. A soft robot for random exploration of terrestrial environments. In Proceedings of the 2018 IEEE International Conference on Robotics and Automation (ICRA), Brisbane, Australia, 21–25 May 2018; IEEE: Piscataway, NJ, USA, 2018; pp. 7492–7497.
31. Li, G.; Wong, T.W.; Shih, B.; Guo, C.; Wang, L.; Liu, J.; Wang, T.; Liu, X.; Yan, J.; Wu, B.; et al. Bioinspired soft robots for deep-sea exploration. *Nat. Commun.* **2023**, *14*, 7097. [CrossRef]
32. Aracri, S.; Giorgio-Serchi, F.; Suaria, G.; Sayed, M.E.; Nemitz, M.P.; Mahon, S.; Stokes, A.A. Soft robots for ocean exploration and offshore operations: A perspective. *Soft Robot.* **2021**, *8*, 625–639. [CrossRef] [PubMed]
33. Calanca, A.; Muradore, R.; Fiorini, P. A review of algorithms for compliant control of stiff and fixed-compliance robots. *IEEE/ASME Trans. Mechatron.* **2015**, *21*, 613–624. [CrossRef]
34. Chen, Y.; Yang, J.; Zhang, X.; Feng, Y.; Zeng, H.; Wang, L.; Feng, W. Light-driven bimorph soft actuators: Design, fabrication, and properties. *Mater. Horizons* **2021**, *8*, 728–757. [CrossRef] [PubMed]
35. Moghadam, A.A.A.; Kouzani, A.; Torabi, K.; Kaynak, A.; Shahinpoor, M. Development of a novel soft parallel robot equipped with polymeric artificial muscles. *Smart Mater. Struct.* **2015**, *24*, 035017. [CrossRef]
36. Abidoye, C.; Grace, D.; Contreras-Esquen, A.; Edwards, A.; Ashuri, T.; Tekes, A.; Amiri Moghadam, A.A. Development of a Novel 3-Universal-Spherical-Revolote Soft Parallel Robot. In Proceedings of the ASME International Mechanical Engineering Congress and Exposition, Columbus, OH, USA, 30 October–3 November 2022; American Society of Mechanical Engineers: New York, NY, USA, 2022; Volume 86670, p. V005T07A022.
37. Lindenroth, L.; Soor, A.; Hutchinson, J.; Shafi, A.; Back, J.; Rhode, K.; Liu, H. Design of a soft, parallel end-effector applied to robot-guided ultrasound interventions. In Proceedings of the 2017 IEEE/RSJ International Conference on Intelligent Robots and Systems (IROS), Vancouver, BC, Canada, 24–28 September 2017; IEEE: Piscataway, NJ, USA, 2017; pp. 3716–3721.
38. Bryson, C.E.; Rucker, D.C. Toward parallel continuum manipulators. In Proceedings of the 2014 IEEE International Conference on Robotics and Automation (ICRA), Hong Kong, China, 31 May–7 June 2014; IEEE: Piscataway, NJ, USA, 2014; pp. 778–785.
39. Hopkins, J.B.; Rivera, J.; Kim, C.; Krishnan, G. Synthesis and analysis of soft parallel robots comprised of active constraints. *J. Mech. Robot.* **2015**, *7*, 011002. [CrossRef]
40. Lilge, S.; Nuelle, K.; Boettcher, G.; Spindeldreier, S.; Burgner-Kahrs, J. Tendon actuated continuous structures in planar parallel robots: A kinematic analysis. *J. Mech. Robot.* **2021**, *13*, 011025. [CrossRef]
41. Nuelle, K.; Sterneck, T.; Lilge, S.; Xiong, D.; Burgner-Kahrs, J.; Ortmaier, T. Modeling, calibration, and evaluation of a tendon-actuated planar parallel continuum robot. *IEEE Robot. Autom. Lett.* **2020**, *5*, 5811–5818. [CrossRef]

42. Wang, Y.; Xu, Q. Design and testing of a soft parallel robot based on pneumatic artificial muscles for wrist rehabilitation. *Sci. Rep.* **2021**, *11*, 1273. [CrossRef] [PubMed]
43. White, E.L.; Case, J.C.; Kramer-Bottiglio, R. A soft parallel kinematic mechanism. *Soft Robot.* **2018**, *5*, 36–53. [CrossRef]
44. Huang, X.; Zhu, X.; Gu, G. Kinematic modeling and characterization of soft parallel robots. *IEEE Trans. Robot.* **2022**, *38*, 3792–3806. [CrossRef]
45. Böttcher, G.; Lilge, S.; Burgner-Kahrs, J. Design of a reconfigurable parallel continuum robot with tendon-actuated kinematic chains. *IEEE Robot. Autom. Lett.* **2021**, *6*, 1272–1279. [CrossRef]
46. Yan, W.; Chen, G.; Tang, S.; Zhang, Z.; Duan, X.; Wang, H. Design of a reconfigurable planar parallel continuum manipulator with variable stiffness. In Proceedings of the Intelligent Robotics and Applications: 14th International Conference, ICIRA 2021, Yantai, China, 22–25 October 2021; Proceedings, Part III 14; Springer: Berlin/Heidelberg, Germany, 2021; pp. 803–813.
47. Yang, Z.; Zhu, X.; Xu, K. Continuum delta robot: A novel translational parallel robot with continuum joints. In Proceedings of the 2018 IEEE/ASME International Conference on Advanced Intelligent Mechatronics (AIM), Auckland, New Zealand, 9–12 July 2018; IEEE: Piscataway, NJ, USA, 2018; pp. 748–755.
48. Garcia, M.; McFall, K.; Tekes, A. Trajectory control of planar closed chain fully compliant mechanism. *J. Mech. Sci. Technol.* **2021**, *35*, 1711–1719. [CrossRef]
49. Lin, H.; Tekes, A.; Tekes, C. Design, development and modelling of single actuated, compliant and symmetrical multi link hopping mechanism. *J. Mech. Sci. Technol.* **2020**, *34*, 555–563. [CrossRef]
50. Tekes, A.; Lin, H.; McFall, K. Design, modelling and experimentation of a novel compliant translational dwell mechanism. *J. Mech. Sci. Technol.* **2019**, *33*, 3137–3145. [CrossRef]
51. Muthusamy, P.K.; Garratt, M.; Pota, H.; Muthusamy, R. Real-time adaptive intelligent control system for quadcopter unmanned aerial vehicles with payload uncertainties. *IEEE Trans. Ind. Electron.* **2021**, *69*, 1641–1653. [CrossRef]
52. Ashuri, T.; Vasquez Mayen, E.; Hamidi, R. A new statistical approach to enhance the performance of model-free optimal controls algorithms. In Proceedings of the 2018 Multidisciplinary Analysis and Optimization Conference, Atlanta, GA, USA, 25–29 June 2018; p. 3421.
53. Tsavnin, A.; Efimov, S.; Zamyatin, S. Overshoot elimination for control systems with parametric uncertainty via a PID controller. *Symmetry* **2020**, *12*, 1092. [CrossRef]
54. Azizkhani, M.; Godage, I.S.; Chen, Y. Dynamic control of soft robotic arm: A simulation study. *IEEE Robot. Autom. Lett.* **2022**, *7*, 3584–3591. [CrossRef]
55. Costanzo, G.T.; Iacovella, S.; Ruelens, F.; Leurs, T.; Claessens, B.J. Experimental analysis of data-driven control for a building heating system. *Sustain. Energy Grids Netw.* **2016**, *6*, 81–90. [CrossRef]
56. Ferri, G.; Munafo, A.; LePage, K.D. An autonomous underwater vehicle data-driven control strategy for target tracking. *IEEE J. Ocean. Eng.* **2018**, *43*, 323–343. [CrossRef]
57. Ashuri, T.; Li, Y.; Hosseini, S.E. Recovery of energy losses using an online data-driven optimization technique. *Energy Convers. Manag.* **2020**, *225*, 113339. [CrossRef]
58. Bruder, D.; Fu, X.; Gillespie, R.B.; Remy, C.D.; Vasudevan, R. Data-driven control of soft robots using Koopman operator theory. *IEEE Trans. Robot.* **2020**, *37*, 948–961. [CrossRef]
59. Peng, X.; Cai, Y.; Li, Q.; Wang, K. Control rod position reconstruction based on K-Nearest Neighbor Method. *Ann. Nucl. Energy* **2017**, *102*, 231–235. [CrossRef]
60. Xu, M.; Wang, P. Evidential KNN-based performance monitoring method for PID control system. In Proceedings of the 2020 5th International Conference on Mechanical, Control and Computer Engineering (ICMCCE), Harbin, China, 25–27 December 2020; IEEE: Piscataway, NJ, USA, 2020; pp. 597–601.
61. Chen, J.; Lau, H.Y. Learning the inverse kinematics of tendon-driven soft manipulators with K-nearest Neighbors Regression and Gaussian Mixture Regression. In Proceedings of the 2016 2nd International Conference on Control, Automation and Robotics (ICCAR), Hong Kong, China, 28–30 April 2016; IEEE: Piscataway, NJ, USA, 2016; pp. 103–107.
62. Xu, W.; Chen, J.; Lau, H.Y.; Ren, H. Data-driven methods towards learning the highly nonlinear inverse kinematics of tendon-driven surgical manipulators. *Int. J. Med. Robot. Comput. Assist. Surg.* **2017**, *13*, e1774. [CrossRef] [PubMed]
63. Zhang, Y.; Huang, P.; Ishibashi, Y.; Okuda, T.; Psannis, K.E. Effect of Neural Network on Robot Position Control Using Force Information. In Proceedings of the 2021 IEEE 9th International Conference on Information, Communication and Networks (ICICN), Xi'an, China, 25–28 November 2021; IEEE: Piscataway, NJ, USA, 2021; pp. 545–549.
64. Young, E.M.; Kuchenbecker, K.J. Implementation of a 6-DOF parallel continuum manipulator for delivering fingertip tactile cues. *IEEE Trans. Haptics* **2019**, *12*, 295–306. [CrossRef] [PubMed]
65. Parsa, F.F.; Moghadam, A.A.A.; Ashuri, T. From Learning Agents to Agile Software: Reinforcement Learning's Transformative Role in Requirements Engineering. In Proceedings of the SoutheastCon 2024, Atlanta, GA, USA, 15–24 March 2024; IEEE: Piscataway, NJ, USA, 2024; pp. 1627–1631.
66. Coy, M.V.C.; Casallas, E.C. Training neural networks using reinforcement learning to reactive path planning. *J. Appl. Eng. Sci.* **2021**, *19*, 48–56.
67. Chen, S.; Dong, J.; Ha, P.; Li, Y.; Labi, S. Graph neural network and reinforcement learning for multi-agent cooperative control of connected autonomous vehicles. *Comput.-Aided Civ. Infrastruct. Eng.* **2021**, *36*, 838–857. [CrossRef]

68. Gillespie, M.T.; Best, C.M.; Townsend, E.C.; Wingate, D.; Killpack, M.D. Learning nonlinear dynamic models of soft robots for model predictive control with neural networks. In Proceedings of the 2018 IEEE International Conference on Soft Robotics (RoboSoft), Livorno, Italy, 24–28 April 2018; IEEE: Piscataway, NJ, USA, 2018; pp. 39–45.
69. Thuruthel, T.G.; Shih, B.; Laschi, C.; Tolley, M.T. Soft robot perception using embedded soft sensors and recurrent neural networks. *Sci. Robot.* **2019**, *4*, eaav1488. [CrossRef] [PubMed]
70. Nadizar, G.; Medvet, E.; Nichele, S.; Pontes-Filho, S. An experimental comparison of evolved neural network models for controlling simulated modular soft robots. *Appl. Soft Comput.* **2023**, *145*, 110610. [CrossRef]
71. Weerakoon, L.; Ye, Z.; Bama, R.S.; Smela, E.; Yu, M.; Chopra, N. Adaptive tracking control of soft robots using integrated sensing skins and recurrent neural networks. In Proceedings of the 2021 IEEE International Conference on Robotics and Automation (ICRA), Xi'an, China, 30 May–5 June 2021; IEEE: Piscataway, NJ, USA, 2021; pp. 12170–12176.
72. Shao, F.; Meng, W.; Ai, Q.; Xie, S.Q. Neural Network Adaptive Control of Hand Rehabilitation Robot Driven by Flexible Pneumatic Muscles. In Proceedings of the 2021 7th International Conference on Mechatronics and Robotics Engineering (ICMRE), Budapest, Hungary, 3–5 February 2021; IEEE: Piscataway, NJ, USA, 2021; pp. 59–63.
73. Bamgbose, S.O.; Li, X.; Qian, L. Neural Network Optimized Controller for Motion and Position Control in Autonomous Systems. In Proceedings of the 2018 IEEE 14th International Conference on Control and Automation (ICCA), Anchorage, AK, USA, 12–15 June 2018; IEEE: Piscataway, NJ, USA, 2018; pp. 823–828.
74. Majumder, A.; Sarkar, D.; Chakraborty, S.; Singh, A.; Roy, S.S.; Arora, A. Neural Network-Based Gain Scheduled Position Control of a Pneumatic Artificial Muscle. In Proceedings of the 2022 IEEE International Conference on Electronics, Computing and Communication Technologies (CONECCT), Bangalore, India, 8–10 July 2022; IEEE: Piscataway, NJ, USA, 2022; pp. 1–6.
75. Ding, S.; Peng, J.; Hou, Y.; Lei, X. Neural Network-based Hybrid Position/Force Tracking Control for Flexible Joint Robot. In Proceedings of the 2020 IEEE International Systems Conference (SysCon), Montreal, QC, Canada, 24 August–20 September 2020; IEEE: Piscataway, NJ, USA, 2020; pp. 1–6.
76. Wang, Y.; Yang, H.; Zhang, P. Position control of planar three-link underactuated manipulator based on wavelet neural network model. In Proceedings of the 2020 39th Chinese Control Conference (CCC), Shenyang, China, 27–30 July 2020; IEEE: Piscataway, NJ, USA, 2020; pp. 387–392.
77. Siciliano, B.; Sciavicco, L.; Chiaverini, S.; Chiacchio, P.; Villani, L.; Caccavale, F. Jacobian-Based Algorithms: A Bridge between Kinematics and Control. In Proceedings of the Special Celebratory Symposium in the Honor of Professor Bernie Roth's 70th Birthday; Citeseer, 2003; pp. 4–35. Available online: https://citeseerx.ist.psu.edu/document?repid=rep1&type=pdf&doi=2f8e8dc8f8058912b9ef5a2c2c247247a326817f (accessed on 15 December 2023).
78. Cheah, C.C.; Kawamura, S.; Arimoto, S. Feedback control for robotic manipulator with an uncertain Jacobian matrix. *J. Robot. Syst.* **1999**, *16*, 119–134. [CrossRef]
79. Cheah, C.C.; Hirano, M.; Kawamura, S.; Arimoto, S. Approximate Jacobian control for robots with uncertain kinematics and dynamics. *IEEE Trans. Robot. Autom.* **2003**, *19*, 692–702. [CrossRef]